

Ag₇Au₆: A 13-Atom Alloy Quantum Cluster**

Thumu Udayabhaskararao, Yan Sun, Nirmal Goswami, Samir K. Pal, K. Balasubramanian, and Thalappil Pradeep*

Dedicated to Professor R. Graham Cooks on the occasion of his 70th birthday

Stable gold cluster molecules of the type Au₁₁,^[1a] Au₁₃,^[1b,c] and Au₅₅,^[1d] have been fascinating and were some of the early molecular nanosystems synthesized. Quantum phenomena such as Coulomb blockade were demonstrated with them.^[2] Unusually intense luminescence and chemical reactivity of molecular clusters or quantum clusters (QCs) of noble metals, for example gold^[3a–c,h] have attracted intense interest in areas such as nanophotonics,^[4] bioimaging,^[5] catalysis,^[6] and others.^[7] In the past several years, some of these clusters have been characterized thoroughly, both theoretically^[8] and experimentally.^[9] Several reports of various core sizes of silver clusters are also known.^[10] However, synthesis of atomically precise alloy QCs of various compositions is a challenge.^[11] Murray et al. synthesized Pd@Au₂₄(SR)₁₈ which was further studied by Negishi et al.^[11b] Negishi et al. isolated PdAu₂₄(SR)₁₈,^[11b] Ag_nAu_{25–n}(SR)₁₈, and (AuAg)₁₄₀(SR)₆₀ (R = organic soluble alkyl/aryl groups) were obtained by simultaneously reducing metal salts in suitable conditions.^[11c,d] There is also a family of well-characterized Ag/Au/Cu cluster complexes^[12] that are different from the metal

core clusters discussed herein. We present the very first experimental investigation of the water-soluble AgAu alloy system belonging to the 13-atom family of clusters by a new synthetic route that reveals a category of materials of structural and electronic complexity that is expected to attract interest in the coming years.

The bimetallic 13-atom QC Ag₇Au₆, which is protected with mercaptosuccinic acid (H₂MSA, or its dianion MSA upon ionization in solution), exhibits well-defined transitions in the absorption profile. This QC is prepared from the Ag_{7,8} cluster (containing a mixture of Ag₇ and Ag₈).^[10d] Synthesis of alloy QCs involves three steps (for details, see the Supporting Information, S1). The various stages of synthesis are shown in Figure 1. First step is the synthesis of polydisperse Ag@H₂MSA nanoparticles followed by the synthesis of Ag_{7,8} clusters by interfacial etching in the second step, as reported previously.^[10d] Addition of an appropriate amount of 10 mM HAuCl₄ to the as-synthesized Ag_{7,8} cluster in the third step yields the alloy cluster (for details see the Experimental Section).

[*] T. Udayabhaskararao, Prof. T. Pradeep
DST Unit of Nanoscience (DST UNS), Department of Chemistry
Indian Institute of Technology, Madras, Chennai 600036 (India)
E-mail: pradeep@iitm.ac

Y. Sun, K. Balasubramanian
College of Science, California State University
East Bay, Hayward, CA 94542 (USA)

N. Goswami, S. K. Pal
Department of Chemical, Biological & Macromolecular Sciences
S. N. Bose National Centre for Basic Sciences
Block JD, Sector III, Salt Lake, Kolkata 700 098 (India)

K. Balasubramanian
Chemistry and Material Science Directorate Lawrence Livermore
National Laboratory, Livermore, CA 94550 (USA)

K. Balasubramanian
Lawrence Berkeley National Laboratory
Berkeley, CA 94720 (USA)

[**] We thank the Department of Science and Technology, Government of India for constantly supporting our research program on nanomaterials. This research was supported in part by the U.S. Department of Energy under grant number DE-FG02-05ER15657 and in part by the Department of Homeland Security's collaborative academic research program. The work at LLNL was performed under the auspices of the U.S. Department of Energy. The authors would like to acknowledge computational support on Lawrence Berkeley Lab's National Energy Research Supercomputers (NERSC).

Supporting information for this article is available on the WWW under <http://dx.doi.org/10.1002/anie.201107696>.

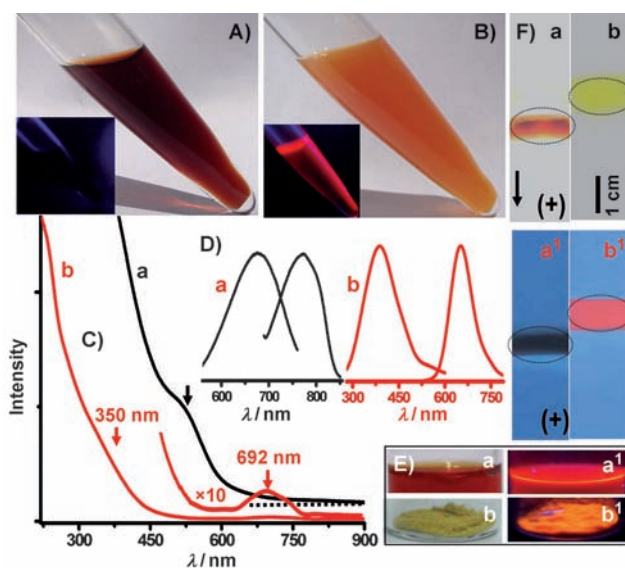


Figure 1. Changes observed during synthesis. A,B) Solutions of Ag_{7,8} (A) and the alloy QC (B) after synthesis under visible light. Insets: the same samples under UV light. C) UV/Vis profile of a) Ag_{7,8} and b) Alloy QC measured in water; arrows indicate the well-defined optical features of the cluster. D) Luminescence spectra of a) Ag_{7,8} and b) alloy QC in water at 300 K. E) Photographs of a,a') alloy QC in water and b,b') in the solid state under visible and UV light. F) Comparison of the PAGE of a,a') Ag₈ and b,b') alloy QC. Photographs of gel in visible (a, b) and UV (a', b') light. Band positions are marked with circles on the gels.

Photographs of $\text{Ag}_{7,8}$ clusters and the alloy QC product after synthesis are shown in Figure 1. During the reaction, the solution becomes turbid and the color changes from reddish brown to orange, indicating the completion of the reaction. A yellowish-white precipitate was removed upon centrifugation and the supernatant appears as a clear reddish yellow solution. The precipitate formed during the reaction is AgCl , as confirmed from XRD and EDAX (Supporting Information, S2). Note that both the thiolate and AgCl are insoluble in water. Finally, the supernatant was lyophilized and a powder sample was obtained for analyzing the cluster in detail. The as-synthesized clusters are stable for months in aqueous phase by storing at low temperatures (below 283 K) and in solid state at room temperature.

The absorption peak from the as-synthesized $\text{Ag}_{7,8}$ cluster at 530 nm (2.34 eV) disappeared within a short reaction time (1 min) and new optical absorption features appear in the next 15 min of reaction with features at 350 (3.54 eV) and 692 nm (1.79 eV). Figure 1C gives the plot of the natural logarithm of the Jacobian factor (details in the Supporting Information) versus wavelength of these clusters, to show the molecular features more clearly. Well-defined absorption features are marked with arrows. Note that Au_{13} cluster also exhibits the peak around 700 nm.^[13] Furthermore, changes in luminescence were observed before and after the reaction, which were attributed to the modifications of the core. For $\text{Ag}_{7,8}$, the excitation and emission maxima are at 670 and 770 nm, whereas for alloy QCs the values are at 390 and 650 nm, respectively (Figure 1D, a,b). Although $\text{Ag}_{7,8}$ cluster emission is weak (quantum yield (QY) of 8×10^{-3}) at room temperature (300 K), for Ag_7Au_6 , the emission intensity is enhanced and the QY was 3.5×10^{-2} . The materials, in both solution and solid states, show bright emission that can be photographed (Figure 1E). Polyacrylamide gel electrophoresis (PAGE) of Ag_8 QC (pre-separated^[10d] sample from $\text{Ag}_{7,8}$) and alloy QC are compared in Figure 1F. They moved to different extent, but as single bands with different mobilities. The mobility of alloy QCs is less than that of Ag_8 QCs, indicating the increase in cluster size. The presence of a single band indicates the formation of one type of cluster in the synthesis. The Ag_8 band does not luminesce brightly at room temperature,^[10d] whereas the alloy QC band shows visible red luminescence under UV light at room temperature (Figure 1F, a¹, b¹). Alloy QCs extracted from the band to water does not show observable shift in the luminescence peak position compared to the crude but there is a slight increase in the intensity (Supporting Information, S3), indicating that both the samples are the same. The cluster appears faintly in TEM but aggregates upon longer electron beam irradiation (Supporting Information, S4) as seen in such clusters.^[3g,10d]

The molecular formula and nature of the monolayer binding are supported by XPS, FTIR, and EDAX (Supporting Information, S5–S7). XPS survey spectrum of Ag_7Au_6 shows the expected elements. The $\text{Au } 4f_{7/2}$ peak at 84.7 eV supports a state intermediate to Au^{I} thiolate (86.0 eV) and Au film (84.0 eV) (Figure 2A, a). There is a slight binding energy (BE) shift of 0.7 eV compared to bulk gold, it is expected for monolayer protected QCs owing to $-\text{S}-\text{Au}-\text{S}-$ staples.^[3] A lower binding energy compared to Au^{I} thiolate is due to the

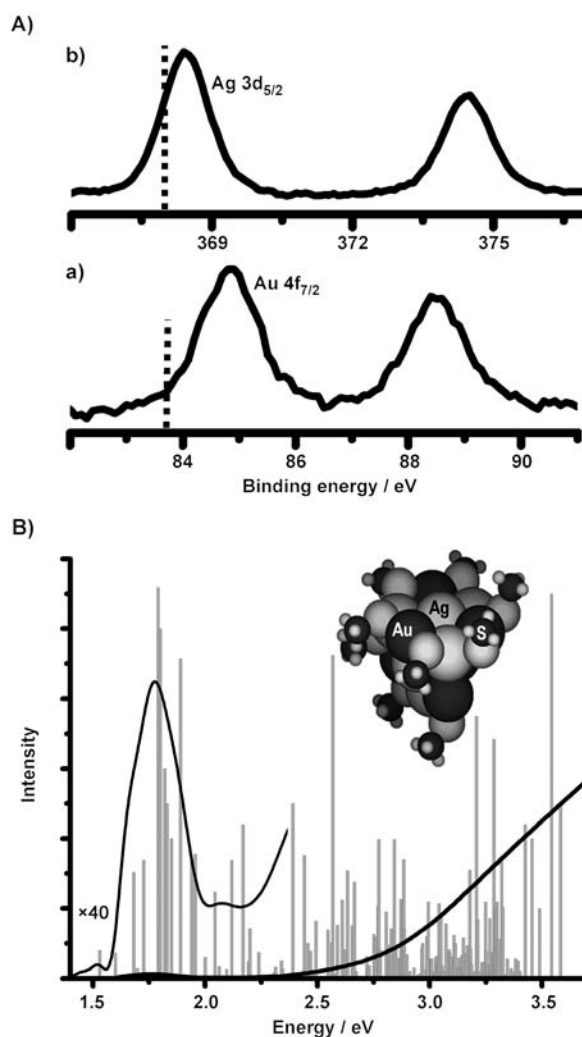


Figure 2. A) XPS spectra in the a) Au 4f and b) Ag 3d regions of $\text{Ag}_7\text{Au}_6(\text{H}_2\text{MSA})_{10}$. Dotted lines indicate the $\text{Au } 4f_{7/2}$ and $\text{Ag } 3d_{5/2}$ positions of the Au^0 and Ag^0 metallic films. B) Simulated absorption spectrum using time-dependent density functional theory (TDDFT). The data are compared with the experimental spectrum (full line). The region in between 1.4 to 2.3 eV is expanded. Inset: One of the optimized structures of the model cluster, $\text{Ag}_7\text{Au}_6(\text{SCH}_3)_{10}$, with which the spectrum was simulated. Ag large light gray, Au black, S small dark gray, CH_3 small light gray.

smaller extent of electron donation from the Au core to thiol ligands in QCs. $\text{Ag } 3d_{5/2}$ (BE of 368.1 eV) supports the Ag^0 state (Figure 2A, b). Note that there is not much difference in BE between Ag^0 and Ag^{I} states, unlike in the case of Au. The $\text{S } 2p_{3/2}$ BE is thiolate-like and a value of 162.0 eV is observed (Supporting Information, S5). An additional $\text{S } 2p_{3/2}$ peak at 164.1 eV observed upon peak fitting may be due to other ligand binding sites or X-ray induced damage.^[14] The total area of the both peaks was used for the estimation of sulfur. An XPS study confirms that a cluster composed of Au and Ag was formed with thiolate protection. ^1H NMR of the cluster is similar to $\text{Ag}_{7,8}$ ^[10d] and Ag_9 ^[10h] clusters protected with MSA, but extent of chemical shift and line broadening are different.

Several direct and indirect methods were used to know the composition of the alloy QC. All the results (discussed

below) compelled us to assign a formula of $\text{Ag}_7\text{Au}_6(\text{MSA})_{10}$ to the cluster. The Ag/Au/S atomic ratio measured in EDAX and XPS were 1:0.82:1.42 and 1:0.84:1.40, respectively in agreement with the ratio expected from the composition of $\text{Ag}_7\text{Au}_6(\text{MSA})_{10}$, namely, 1:0.86:1.43 (normalized with respect to Ag). Elemental analysis showed that the cluster contains an organic fraction of about 43.7% (C 14.03, H 1.76, O 18.68, S 9.34%), in good agreement with calculated value of 43.4%. Au and Ag were independently estimated by ICP AES and were found to be 35.2% and 23.4%, respectively (expected 34.4 and 22.0%, respectively).

We have investigated the geometric and electronic structures of the model system, $\text{Ag}_7\text{Au}_6(\text{SCH}_3)_{10}$ theoretically (for details, see the Supporting Information, S1). The Ag_7Au_6 core was fully optimized without any symmetry restrictions and then the ligands were added, yielding $\text{Ag}_7\text{Au}_6(\text{SCH}_3)_{10}$; the structure was optimized again. One of the possible structures is presented in Figure 2B, which originated from the Ag_7Au_6 core of C_{2v} symmetry, with the thiolates bonded in a bridged form, $-\text{Au}/\text{Ag}-\text{SR}-\text{Au}/\text{Ag}-$. The structure has a distorted icosahedral core. The simulated absorption spectra of this structure obtained by time-dependent density functional theory (TDDFT) agreed well with the experimental results, showing several excited states with relatively strong oscillator strengths coinciding with the experimentally measured values of 350 and 692 nm. There are a few other structures of similar energies as well (Supporting Information, S8).

Electrospray ionization mass spectrometry (ESI-MS) measurements of the as-prepared cluster does not show characteristic peaks owing to its decomposition at capillary temperatures. This is not surprising as the cluster in aqueous medium starts degrading to thiolates around 313 K. Similar degradation was also observed for Ag_9 QCs.^[10b] To create charged droplets at minimum capillary temperatures in ESI, we performed partial ligand exchange and transferred the cluster to the organic medium (Supporting Information, S1). The exchanged product in toluene shows absorption peaks at 350 and 690 nm that match with the absorption profiles of the MSA protected cluster, thus indicating that the cluster core is the same under ligand exchange.^[3h] Luminescence spectra also did not show change, suggesting the same (Supporting Information, S9). It was important that the ligand exchange was partial so that some H_2MSA ligands are also present on the cluster that could yield carboxylate ions upon ionization.

A mass spectrum of PET- (phenylethanethiol) exchanged clusters in toluene/methanol (1:1, v/v) mixture (Figure 3) showed characteristic signatures that correspond to these clusters. Several aspects of the mass spectrum support a chemical composition of $\text{Ag}_7\text{Au}_6(\text{ligand})_{10}$ for the cluster. First, the observed isotope pattern matches perfectly with the theoretical prediction. Second, the peak positions of the ions are in perfect agreement, and third, the mass spectral series terminate exactly after six tropylium losses, as only six PET ligands are exchanged and they only can show these losses. The spectrum is seen only in the negative-ion mode, as H_2MSA is a dicarboxylic acid (giving MSA dianion after complete ionization). This assignment also matches well with the HT exchanged cluster (Supporting Information, S10). The

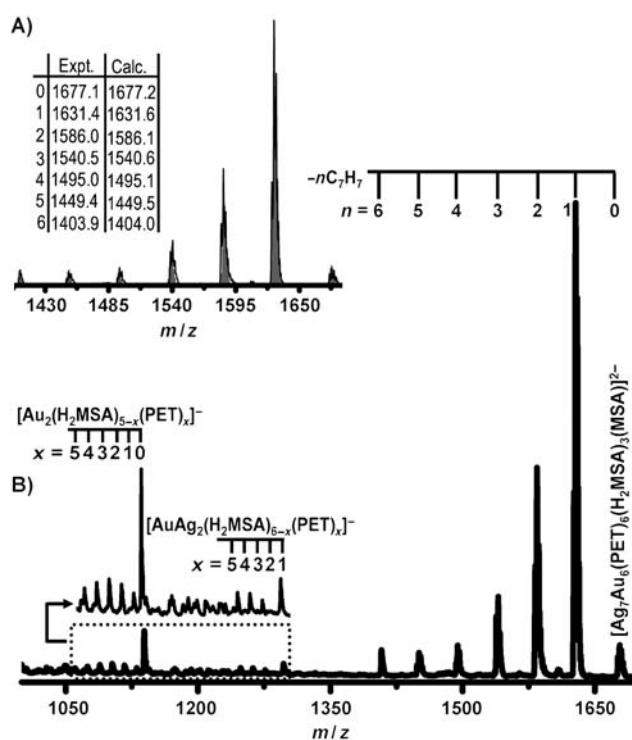


Figure 3. ESI MS spectrum of the PET-exchanged cluster in the negative-ion mode and in the region m/z 1000–1700. Sequential loss of tropylium ($n=0, 1, 2, \dots, 6$) was seen in ionization. The clusters show substitution of six ligands. The calculated isotope pattern is shown as gray under the experimental peak envelope in inset A. Inset B shows fragments.

lower-mass (m/z 1000–1300) peaks are from the smaller fragments owing to fragmentation. The peaks in the series are separated by m/z 12 and are due to the exchange of PET (MW 138.20) for H_2MSA (MW 150.15), as shown in Figure 3B.

Several experimental results^[3h,17] suggest that the position and intensity of the emission depends on the type of the protecting ligand. The luminescence intensity was a function of ligand protection; it followed the trend $\text{PET} > \text{OT} > \text{HT}$. The ligands influence the luminescence emission as observed in the Au_{25} system.^[3c,15] $\text{Ag}_7\text{Au}_6(\text{MSA})_{10}$ shows enhancement in luminescence upon phase transfer to toluene using phase transfer agent TOABr (Supporting Information, S11).^[3c,10k] The average luminescence lifetimes for these samples before and after phase transfer were 1.0 and 10.0 ns, respectively. The percentage of the faster component decreased by 30% after phase transfer; this is a consequence of reduction in non-radiative decay.^[3b] This kind of reduction is also observed for ligand-exchanged products (excitation at 409 nm and detection at 650 nm) of $\text{Ag}_7\text{Au}_6(\text{PET})_x(\text{H}_2\text{MSA})_{10-x}$, $\text{Ag}_7\text{Au}_6(\text{HT})_x(\text{H}_2\text{MSA})_{10-x}$, and $\text{Ag}_7\text{Au}_6(\text{OT})_x(\text{H}_2\text{MSA})_{10-x}$. Their average luminescence lifetimes are in the order $\text{PET} > \text{OT} > \text{HT}$ (11.9 > 7.9 > 4.8 ns). All of the samples exhibit a tri-exponential decay. There seems to be a pattern of average lifetime that may depend on the electron-donating property of the ligands.^[15] Lifetimes of the cluster before and after phase transfer and ligand exchange are given in the Supporting Information, S12.

From our previous reports, QCs undergo decomposition in presence of free metal ions, especially Au^{3+} .^[3f] It is also known that a metal-core galvanic exchange reaction was successful when Ag/Pd/Cu nanoparticles were treated with $\text{Au}^{\text{I}}\text{SR}$ instead of Au^{3+} .^[16] We propose that the mechanism of formation of the bimetallic clusters involves the reaction of Au^{3+} with unbound H_2MSA or Ag thiolate, forming Au^{I} -thiolate, which reacts with the $\text{Ag}_{7,8}$ clusters to form the alloy cluster. Indeed, the addition of Au^{I} thiolate to pure PAGE-separated Ag_8 clusters also forms the desired product. The addition (of more than the optimized amount) of HAuCl_4 to crude $\text{Ag}_{7,8}$ clusters produces plasmonic nanoparticles, and further addition leads to charge neutralization according to the Schultze–Hardy rule,^[18] resulting in coagulation and settling. This residue was analyzed using TEM, SEM, and a luminescence image, which shows the presence of tubular arrangement of nanoparticles (Supporting Information, S13). It is expected that thiolate acts as a template for this arrangement of nanoparticles (note that thiolate structures are layered).^[17] Several systematic control experiments were carried out to improve the yield of the alloy cluster and to arrive at this simplified procedure (Supporting Information, S14).

It is important to have various specific ingredients to form the cluster. Direct addition of HAuCl_4 to Ag^{I} thiolate or to PAGE-purified Ag_8 separately did not produce the desired product. In the former case, it is understood that there is no driving force for the reduction of Au^{3+} . In the latter case, the addition of HAuCl_4 to pure Ag_8 leads to the decomposition of the cluster and simultaneous reduction of Au^{3+} . This results in the formation of differently shaped gold–silver plasmonic nanomaterials (Supporting Information, S15, S16). This kind of decomposition reaction was observed in purified crude mixture of clusters (in the absence of thiolates + unbound H_2MSA ; for details see the Supporting Information, S1), indicating that both the clusters are playing a similar role in the reaction. However, a detailed mechanism of the formation of alloy clusters requires extensive investigations.

Similar experiments were carried out by taking glutathione-protected clusters. For this case, interfacial etching of polydisperse Ag@MSA was carried out with glutathione to produce Ag@SG QCs. The addition of HAuCl_4 to crude Ag@SG gives a red luminescent alloy QC with a distinct absorption profile. The protection of glutathione was confirmed by NMR spectroscopy (Supporting Information, S17). The extent of reaction to other kinds of silver QCs was also checked. For that we selected well-characterized, atomically pure $\text{Ag}_9(\text{MSA})_7$.^[10b] There are changes in the absorption profile during the reaction between $\text{Au}^{\text{I}}\text{MSA}$ and Ag_9 QCs. Reactions are very sensitive to the concentrations of reactants, and diverse clusters of varying properties can be prepared (Supporting Information, S18). Detailed experimental characterization of the clusters is beyond the scope of this work and will be reported separately.

In summary, a new 13-core Ag_7Au_6 QC was synthesized by a galvanic exchange reaction, starting from $\text{Ag}_{7,8}$ precursor. It exhibits quantum confinement in the absorption profile. The cluster is pure as confirmed by PAGE and was characterized by UV/Vis, FTIR, luminescence, TEM, XPS, SEM/EDAX,

and ESI MS. Possible structures have been investigated theoretically. The extension of this reaction to produce various alloy QCs was carried out by taking $\text{Ag}_{\text{QC}}\text{@SG}$ and $\text{Ag}_9(\text{MSA})_7$ as examples.

Experimental Section

Synthesis of alloy QCs: To of as-synthesized crude $\text{Ag}_{7,8}$ cluster (3.0 mL reddish brown solution in water containing $\text{Ag}_8 + \text{Ag}_7$ + thiolate) without washing, containing 10.0 mg of clusters, HAuCl_4 (6.0 mL, 10 mM) was added and stirred for 15 min at 293 K. The formation of the cluster was checked by the appearance of luminescence under UV light which was absent at 300 K for the parent clusters. The resultant solution was centrifuged to remove AgCl and thiolate. The reaction product was precipitated by the addition of excess methanol and washed to remove dissolved reactants such as H_2MSA or other ions. The cluster product was obtained by solvent evaporation using a rotary evaporator and the material was stored in the laboratory atmosphere. Analytical and computational methods are described in the Supporting Information, S1.

Received: November 1, 2011

Published online: January 20, 2012

Keywords: alloy clusters · ESI-MS · luminescence · quantum clusters · silver

- [1] a) P. A. Bartlett, B. Bauer, S. J. Singer, *J. Am. Chem. Soc.* **1978**, *100*, 5085; b) C. E. Briant, B. R. C. Theobald, J. W. White, C. K. Bell, D. M. P. Mingos, A. J. Welch, *J. Chem. Soc. Chem. Commun.* **1981**, 201; c) J. W. A. van der Velden, F. A. Vollenbroek, J. J. Bour, P. T. Beurskens, J. M. M. Smits, W. P. Bosman, *Recl. J. R. Neth. Chem. Soc.* **1981**, *100*, 148; d) G. Schmid, R. Pfeil, R. Boese, F. Bandermann, S. Meyer, G. H. M. Calis, J. W. A. Van der Velden, *Chem. Ber.* **1981**, *114*, 3634.
- [2] L. F. Chi, M. Hartig, T. Drechsler, T. Schwaack, C. Seidel, H. Fuchs, G. Schmid, *Appl. Phys. A* **1998**, *66*, S187.
- [3] a) R. Jin, *Nanoscale* **2010**, *2*, 343, and references therein; b) P. L. Xavier, K. Chaudhari, P. K. Verma, S. K. Pal, T. Pradeep, *Nanoscale* **2010**, *2*, 2769; c) M. A. Habeeb Muhammed, P. K. Verma, S. K. Pal, R. C. Arun Kumar, S. Paul, R. V. Omkumar, T. Pradeep, *Chem. Eur. J.* **2009**, *15*, 10110; d) E. S. Shibu, B. Radha, P. K. Verma, P. Bhyrappa, G. U. Kulkarni, S. K. Pal, T. Pradeep, *ACS Appl. Mater. Interfaces* **2009**, *1*, 2199; e) H. Qian, Y. Zhu, R. Jin, *J. Am. Chem. Soc.* **2010**, *132*, 4583; f) M. A. Habeeb Muhammed, T. Pradeep, *Chem. Phys. Lett.* **2007**, *449*, 186; g) P. Ramasamy, S. Guha, E. S. Shibu, T. S. Sreeprasad, S. Bag, A. Banerjee, T. Pradeep, *J. Mater. Chem.* **2009**, *19*, 8456; h) E. S. Shibu, M. A. Habeeb Muhammed, T. Tsukuda, T. Pradeep, *J. Phys. Chem. C* **2008**, *112*, 12168.
- [4] C. L. Haynes, A. D. McFarland, L. L. Zhao, R. P. Van Duyne, G. C. Schatz, L. Gunnarsson, J. Prikulis, B. Kasemo, M. Kall, *J. Phys. Chem. B* **2003**, *107*, 7337.
- [5] a) A. M. Gobin, M. H. Lee, N. J. Halas, W. D. James, R. A. Drezek, J. L. West, *Nano Lett.* **2007**, *7*, 1929; b) A. Verma, O. Uzun, Y. H. Hu, Y. Hu, H. S. Han, N. Watson, S. L. Chen, D. J. Irvine, F. Stellacci, *Nat. Mater.* **2008**, *7*, 588.
- [6] Y. Zhu, H. Qian, B. A. Drake, R. Jin, *Angew. Chem.* **2010**, *122*, 1317; *Angew. Chem. Int. Ed.* **2010**, *49*, 1295.
- [7] a) G. Ramakrishna, O. Varnavski, J. Kim, D. Lee, T. Goodson, *J. Am. Chem. Soc.* **2008**, *130*, 5032; b) J. I. Gonzalez, T.-H. Lee, M. D. Barnes, Y. Antoku, R. M. Dickson, *Phys. Rev. Lett.* **2004**, *93*, 147402; c) M. A. Habeeb Muhammed, A. K. Shaw, S. K. Pal,

- T. Pradeep, *J. Phys. Chem. C* **2008**, *112*, 14324; d) N. Sakai, T. Tatsuma, *Adv. Mater.* **2010**, *22*, 3185.
- [8] H. Häkkinen, *Chem. Soc. Rev.* **2008**, *37*, 1847.
- [9] a) P. D. Jadzinsky, G. Calero, C. J. Ackerson, D. A. Bushnell, R. D. Kornberg, *Science* **2007**, *318*, 430; b) M. W. Heaven, A. Dass, P. S. White, K. M. Holt, R. W. Murray, *J. Am. Chem. Soc.* **2008**, *130*, 3754.
- [10] a) O. M. Bakr, V. Amendola, C. M. Aikens, W. Wenselers, R. Li, L. D. Negro, G. C. Schatz, F. Stellacci, *Angew. Chem.* **2009**, *121*, 6035; *Angew. Chem. Int. Ed.* **2009**, *48*, 5921; b) Z. Wu, E. Lanni, W. Chen, M. E. Bier, D. H. Ly, R. Jin, *J. Am. Chem. Soc.* **2009**, *131*, 16672; c) N. Nishida, H. Yao, T. Ueda, A. Sasaki, K. Kimura, *Chem. Mater.* **2007**, *19*, 2831; d) T. Udaya Bhaskara Rao, T. Pradeep, *Angew. Chem.* **2010**, *122*, 4017; *Angew. Chem. Int. Ed.* **2010**, *49*, 3925; e) H. Yao, M. Saeki, K. Kimura, *J. Phys. Chem. C* **2010**, *114*, 15909; f) K. V. Mrudula, T. Udaya Bhaskara Rao, T. Pradeep, *J. Mater. Chem.* **2009**, *19*, 4335; g) N. Cathcart, V. Kitaev, *J. Phys. Chem. C* **2010**, *114*, 16010; h) T. U. B. Rao, B. Nataraju, T. Pradeep, *J. Am. Chem. Soc.* **2010**, *132*, 16307; i) S. Kumar, M. D. Bolan, T. P. Bigioni, *J. Am. Chem. Soc.* **2010**, *132*, 1314; j) I. Díez, R. H. A. Ras, *Nanoscale* **2011**, *3*, 1963; k) I. Díez, H. Jiang, R. H. A. Ras, *ChemPhysChem* **2010**, *11*, 3100; l) I. Díez, M. Pusa, S. Kulmala, H. Jiang, A. Walther, A. S. Goldmann, A. H. E. Muller, O. Ikkala, R. H. A. Ras, *Angew. Chem.* **2009**, *121*, 2156; *Angew. Chem. Int. Ed.* **2009**, *48*, 2122.
- [11] a) C. A. Fields-Zinna, M. C. Crowe, A. Dass, J. E. F. Weaver, R. W. Murray, *Langmuir* **2009**, *25*, 7704; b) Y. Negishi, W. Kurashige, Y. Niihori, T. Iwasa, K. Nobusada, *Phys. Chem. Chem. Phys.* **2010**, *12*, 6219; c) Y. Negishi, T. Iwai, M. Ide, *Chem. Commun.* **2010**, *46*, 4713; d) C. Kumara, A. Dass, *Nanoscale* **2011**, *3*, 3064; e) H. Qian, E. Barry, Y. Zhu, R. Jin, *Acta Phys. Chim. Sin.* **2011**, *27*, 513.
- [12] a) G. M. Concepcion, A. Laguna, *Chem. Soc. Rev.* **2008**, *37*, 1952; b) A. Laguna, T. Lasanta, J. M. López-de-Luzuriaga, M. Monge, P. Naumo, M. E. Olmos, *J. Am. Chem. Soc.* **2010**, *132*, 456.
- [13] L. D. Menard, S.-P. Gao, H. Xu, R. D. Twisten, A. S. Harper, G. Wang, A. D. Douglas, J. C. Yang, A. I. Frenkel, R. G. Nuzzo, R. W. Murray, *J. Phys. Chem. B* **2006**, *110*, 12874.
- [14] M. S. Bootharaju, T. Pradeep, *Langmuir* **2011**, *27*, 8134.
- [15] Z. Wu, R. Jin, *Nano Lett.* **2010**, *10*, 2568.
- [16] a) Y.-S. Shon, G. B. Dawson, M. Porter, R. W. Murray, *Langmuir* **2002**, *18*, 3880; b) T. Huang, R. W. Murray, *J. Phys. Chem. B* **2003**, *107*, 7434.
- [17] a) N. Sandhyarani, M. P. Antony, G. Panneer Selvam, T. Pradeep, *J. Chem. Phys.* **2000**, *113*, 9794; b) I. G. Dance, K. J. Fisher, R. M. H. Banda, M. L. Scudder, *Inorg. Chem.* **1991**, *30*, 183.
- [18] W. Nowicki, G. Nowicka, *J. Chem. Educ.* **1994**, *71*, 624.